CHAPTER-II : PREPARATION OF FERRITES AND X-RAY DIFFRACTION STUDIES

A]   Method of Preparation

B]   X-ray Diffraction

C]   Determination of Curie Temperature

ΛΛΔΛΛ

Method of Preparation

Introduction

2.1   Simple, mixed and substitutional ferrites can be prepared by various methods.[1,2,3]

We have prepared the ferrites by sintering of the oxides which is known as ceramic method.[4]

2.2   Mechanism of Solid State Reaction

The mechanism is discussed on the basis of diffusion of components involving divalent metal oxides MO and Fe_2O_3. At the initial state there is only phase boundary between reactants. After the nucleation of the ferrites, the boundary is replaced by two different phase boundaries - one between MO and Ferrite MFe_2O_4 and other between Fe_2O_4 and MFe_2O_4. In this case reaction further takes place by transport of reactants through the ferrite phase. Transfer of MFe_2O_4 can take place by three ways. According to Wanger[5,6] only cation migration takes place in the opposite directions, while oxygen ions are stationary. In the second model anions diffuse. In this type of diffusion cation diffusion is compensated by diffusion of anions. According to third mechanism iron diffuses through the Ferrite layer in a reduced state Fe^{2+}. In such a case oxygen is transported through the gas phase, being given off at MFe_2O_4/Fe_2O_3 interface and taken up again at MO/MFe_2O_4 boundary.

2.3   The General Formula

The general formula of our ferrite system is $Zn_xMg_{1-x}Fe_2O_4$, where $x = 0, 0.2, 0.4, 0.6, 0.8, 1.$

2.4   Raw Materials

AR grade Fe_2O_3, Zno and MgO were used to prepare ferrite.

2.5   Weighing

The oxides were weighed on a single pan balance of least count 10^{-5} g and mixed according to their molecular weight percentages.

2.6   Pre-sintering

The weighed oxides were thoroughly mixed, finely divided in agate morter in AR grade acetone base. The mixture was allowed to dry in air and carefully transferred to a clean dry platinum crucible and presintered in a glo bar furnace at $600^{\circ}C$ for about 20 hours. The samples were cooled in the furnace at the rate of $80^{\circ}C$ per hour by reducing current gradually. A chromel alumel thermocouple and digital multimeter were used to measure the temperature.

2.7   The samples were then finally powdered by grinding for three hours in an agate morter. The samples were then sieved,

2.8   Pellet Formation

The samples were powdered and pillets of 1 cm diameter were prepared by applying pressure of 10 tans/inch^2 for about 15 minutes 10% solution of polyvenyl acetate was used as the binder.

2.9   Final sintering

The pellets so prepared were sintered in the glo-bar furnace at 1200°C for about 36 hours. The samples were cooled at the rate of 80°C/hour.

(B)   X-ray Diffraction Study

2.10   Introduction

To confirm the formation of Ferrite samples and characterisation of crystal structure XRD patterns have been recorded. The peaks of the diffractogram are indexed, the lattice constants a and d values have been calculated. The results are discussed.

2.11   Details of Diffractometer

i)   Target used CoKα

ii)   Wavelength 1.79021 ^{o}A

iii)   Rate of scanning 2° per minute

iv)   Range of 2θ 10 to 100

v)   Operating voltage 30 kV

Zn$_{0.2}$Mg$_{0.8}$Fe$_2$O$_4$

111, 220, 311, 400, 422, 511/333, 440

Mg$_{0.4}$Zn$_{0.6}$Fe$_2$O$_4$

111, 220, 311, 400, 422, 511/333, 440

Zn$_{0.8}$Mg$_{0.2}$Fe$_2$O$_4$

111, 220, 311, 222, 400, 422, 511/333, 440
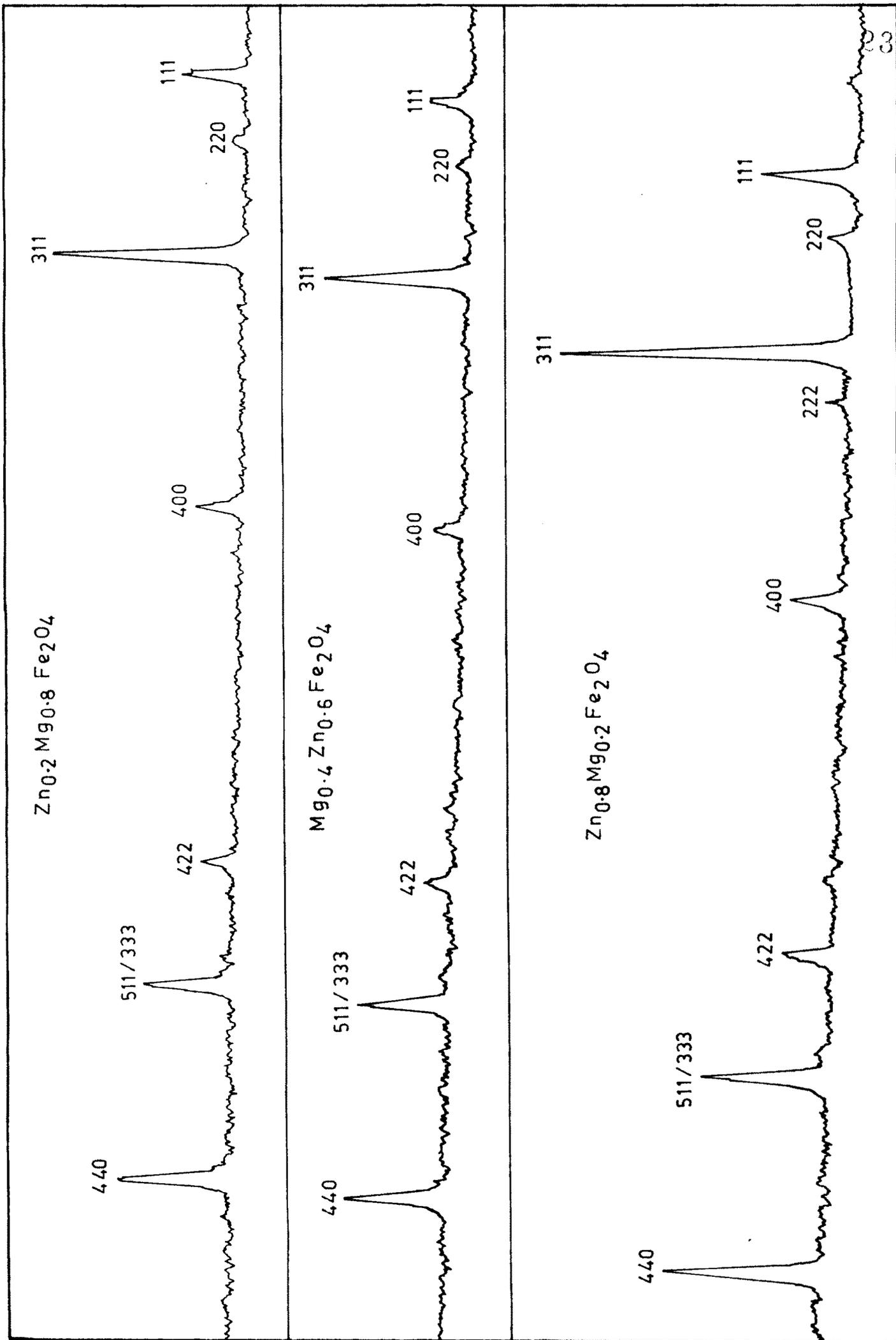
X-RAY DIFFRACTION STUDIES

vi) Operating current 30 mA

vii) Slit 0.3 mm

Indexing of the peaks in the diffraction patterns for a cubic lattice, the interplaner distance d(hkl), lattice parameter a and millar indices (hkl) are related by[7]

$$d_{hkl} = \frac{a}{\sqrt{h^2 + k^2 + l^2}} \tag{1}$$

According to Bragg's law

$$2d_{hkl} \sin\theta_{hkl} = n\lambda \tag{2}$$

for n = 1

$$2d_{hkl} \sin\theta_{hkl} = \lambda$$

where λ = 1.79021 $^{\circ}A$ for CoKα radiation

The peak of 100% height corresponds to the plane (3 11). So the lattice parameter 'a' in this case is calculated by using the relation (2). For other planes the (hkl) values were determined by the usual procedure[8] and the peak indexed.

2.12 Result and Discussion

The diffraction maxima have been indexed and indices tallied with those expected for spinel structure. The reflections observed are (1,1,1), (2,2,0), (3,1,1), (2,2,2), (4,0,0), (4,2,2), (5,1,1) or (3,3,3) and (4,4,0). This corresponds to the allowed values of reflection for cubic spinel structure.[8] The observed

and calculated d values miller indices with lattice parameter are presented in the Tables (Table Nos. 2.1 to 2.6).

Fig. 2.1 shows compositional variation of the lattice parameter a A° with the content of zinc for ferrite system $Mg_xZn_{1-x}Fe_2O_4$. It is seen that as the content of zinc is increased the lattice parameter increases almost in a linear fashion. The lattice parameter is minimum for $Mg\ Fe_2O_4$ $(8.38A^{\circ})$ and maximum for $ZnFe_2O_4$ $(8.44\ A^{\circ})$. These values are in close agreement with those reported earlier.[9,10] The compositional variation of lattice parameter shows that Vegard's law is obeyed.

Table No. 2.7

[11]

Ion	Mg	Zn
Ionic radius	$0.75A^{\circ}$	$0.83A^{\circ}$

From Table No. 2.7 it is seen that the ionic volume for Mg^{++} is smaller than that for Zn^{++}. When zinc is substituted for Mg^{++}, this trend is expected.

It is also observed that on quenching the samples from $800^{\circ}C$ there is no change in either the structure or the lattice parameter. Therefore, XRD patterns for quenched samples have been excluded.

In Figs. 2.2 and 2.3 variation of average bond lengths R_A and R_B against the content of Zn in the system $Zn_xMg_{1-x}Fe_2O_4$

is shown. The values of R_A and R_B are calculated by using the
relations given below.[13]

$$R_A = a \sqrt{3} \left(\frac{1}{8} + \delta \right)$$

and

$$R_B = a \sqrt{\frac{1}{16} - \frac{\delta}{2} + 3\delta^2}$$

where R_A is the shortest distance between A site cation and
oxygen ion and R_B is the shortest distance between B site cation
and oxygen ion and $= u-0.375$, the deviation from U value. The
U values used for calculations are from the data already reported
for these ferrites[14] from Fig. 2.2 it is seen that on the content
of Zn in the system $Zn_xMg_{1-x}Fe_2O_4$ increases, the value of R_A also
increase. A linear relation is exhibited by the compositional
variation of R_A. The value of R_A is minimum for $MgFe_2O_4$ and
maximum for $Zn Fe_2O_4$.

The increase of average bond length R_A can be associated
with the increase in the lattice parameter 'a' with the content
of Zn. As content of Zn in the system $Zn_xMg_{1-x}Fe_2O_4$ increases,
presence of Zn^{+2} ions on A-site increases, since $ZnFe_2O_4$ is a
normal spinel and Zn^{+2} occupies A-site only, the bond length R_A
increases with more content of Zn^{+2} in the system.

Levine[15] in his work on bond susceptibility on spinels
has shown that there exists an inverse relationship between the
covalent character of spinel and the bond length. From Fig. 2.3

27

it is seen that as the content of Zn in the ferrite system $Zn_xMg_{1-x}Fe_2O_4$ increases the bond length R_B decreases. The value of R_B is maximum for $MgFe_2O_4$ and minimum for $ZnFe O$. Thus, (on the B-site) the compositional variation of R_B suggests that. the ionocovalent character increases with the content of Zn. As Zn^{+2} occupies A-site only and bonding between Fe^{+3} ions on B-site being ionic, it is the partial ionic bonding between Mg^{+2} ions on B-site that lends iono-covalent character to the mixed system. The nature and variation of the bonding can be discussed on the basis of crystal field splitting as suggested by Dunitz and Orgel.[16]

In Fig. 2.4 compositional variation of the Curie temperatures (Tc) is shown. It is seen that there is a similarity in the variation of experiments and theoretical values of Curie temperature. However, there is a considerable deviation in the theoretical value of Tc and experimental value of Tc. The theoretical values of Tc are for all the samples greater than the experimental values of Tc. Theoretical values of Tc are evaluated on the assumption that all the $Mg_{0.9}$ ions stay on B-site. Thus, the deviation in the values of Tc clearly indicates that there is a migration of Mg^{+2} from B-site to A-site.

The variation of Tc with the content of Zn is nonlinear. Tc has maximum value for $MgFe_2O_4$ and minimum value for $Zn_{.6}Mg_{.4}Fe_2O_4$. For the samples $Zn_{.8}Mg_{.2}Fe_2O_4$ and $ZnFe_2O_4$ values

of Tc could not be computed which is expected. The non-linear compositional variation of Tc indicates that with the addition of Zn, triangular type of spin arrangements are favoured. As the Zn content increases the degree of the strength of A-B interaction decreases.[17] This is evidenced by the lowering of Tc values with the content of Zn upto 60 per cent. For the samples of $Zn_{.8}Mg_{.2}Fe_2O_4$ and $AZnFe_2O_4$ the A-B interaction no longer favours and the parallel arrangements of spins of B-B sub-lattice. Hence, these samples become non-magnetic and do not show Tc above room temperature.

Apparatus and Determination of Curie Temperature

The procedure for experimental determination of Curie temperatures is explained in detail beneath. Method of determination of Curie temperature is already suggested by Loria et al.[12] However, we have improved upon this method for it has its own shortcomings. The pellets as well as the core of electromagnets are exposed to hot environment leading to the short circuit, due to which damage is caused to the enamel of the wire of the electromagnet. We have not exposed the core of the electromagnet directly to the furnace temperature. Instead induction method is employed to magnetise the specimen bar to which pellet was attached. Cromel-alumel thermocouple and digital multimeter were used for temperature recording to accuracy of less than 5 per cent.

The Curie temperatures are given in Table No. 2.8 for the slow cooled as well as the samples quenched from $800^{\circ}C$. It is observed that:

1) Curie temperatures are lowered on addition of zinc and

11) Curie temperatures of slow cooled samples are more than those for quenched samples.

Table 2.1

$MgFe_2O_4$ a = 8.38 A°

hkl	d(observed) A°	d (calculated) A°
111	4.81	4.83
220	2.95	2.96
311	2.52	2.51
400	2.09	2.07
422	1.71	1.71
511/333	1.61	1.61
440	1.48	1.48

Table 2.2

$Zn_{.2}Mg_{.8}Fe_2O_4$ a = 8.39 A°
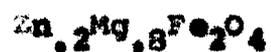
hkl	d(observed) A°	d(calculated) A°
111	5.57	5.57
220	3.10	3.11
311	2.61	2.60
400	2.10	2.10
422	1.68	1.69
511/333	1.59	1.59
440	1.47	1.46

Table 2.3

$Zn_{.4}Mg_{.6}Fe_2O_4$ a = 8.41 A°
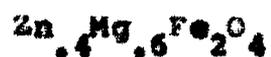
hkl	d(observed) A°	d(calculated) A°
111	5.78	5.78
220	3.13	3.13
311	2.62	2.62
400	2.10	2.10
422	1.68	1.69
511/333	1.56	1.57
440	1.44	1.44

Table 2.4

$Zn_{.6}Mg_{.4}Fe_2O_4$ $a = 8.42 \, A^o$
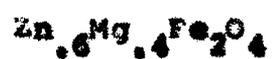
hkl	d(observed) A^o	d(calculated) A^o
111	4.80	4.80
220	2.88	2.88
311	2.45	2.45
222	2.35	2.35
400	2.00	2.00
422	1.65	1.65
511/333	1.56	1.56
440	1.43	1.43

Table 2.5

$Zn_{.8}Mg_{.2}Fe_2O_4$ $a = 8.43 \, A^o$
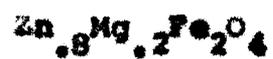
hkl	d(observed) A^o	d(calculated) A^o
111	5.26	5.26
220	3.05	3.05
311	2.57	2.57
222	2.45	2.45
400	2.10	2.10
422	1.71	1.71
511/333	1.60	1.61
440	1.47	1.47

Table 2.6

ZnFe$_2$O$_4$ a = 8.44 A$^\circ$

hkl	d(observed) A$^\circ$	d(calculated) A$^\circ$
111	4.89	4.89
220	2.99	2.99
311	2.56	2.56
222	4.48	4.48
400	2.11	2.11
422	1.72	1.72
511/333	1.62	1.62
440	1.50	1.50

Table 2.8

Lattice parameter, Curie temperature, for
$Zn_xMg_{1-x}Fe_2O_4$ system

No.	Composition	Lattice parameter	Curie temperature		Quenched sample
			Theoretical	Experimental	
1	$MgFe_2O_4$	8.38 Å°	450°C	482°C	435°C
2	$Mg_{.8}Zn_{.2}Fe_2O_4$	8.39 Å°	419°C	375°C	360°C
3	$Mg_{.6}Zn_{.4}Fe_2O_4$	8.41 Å°	325°C	282°C	245°C
4	$Mg_{.4}Zn_{.6}Fe_2O_4$	8.42 Å°	162°C	145°C	120°C
5	$Mg_{.2}Zn_{.8}Fe_2O_4$	8.43 Å°	-	Below room temp.	-
6	$ZnFe_2O_4$	8.44 Å°	-	-	-

Fig. 2·1

Fig. 2·2

Fig. 2·3

Fig. 2·4

1   Electromagnet
2   Porcelin sheet
3   Furnace
4   Lid
5   Soft iron piece
6   Thermocouple
7   Pellet
8   Metal lid
9   Digital voltmeter

A

mV

9

1
2
3
4
5
6
7
8
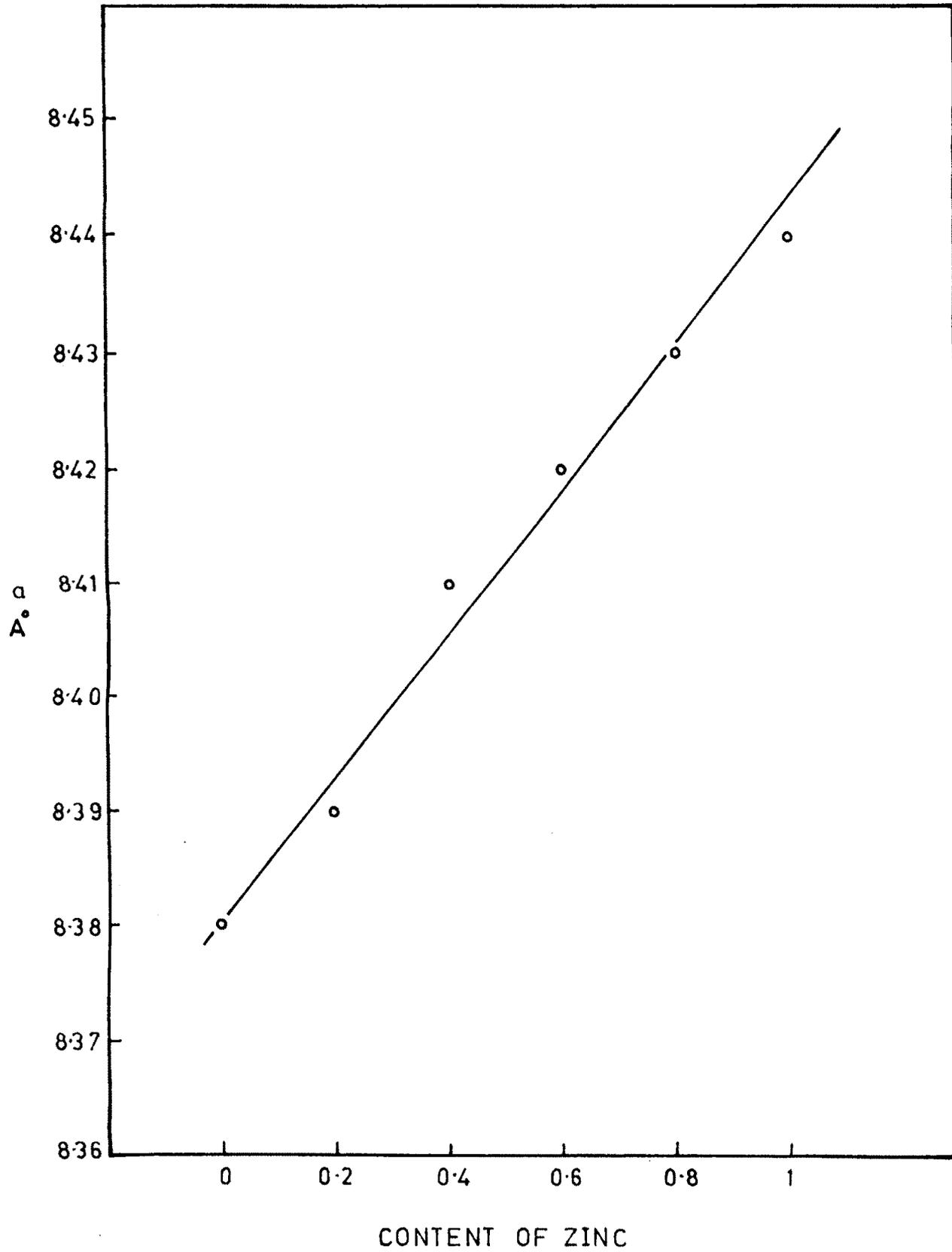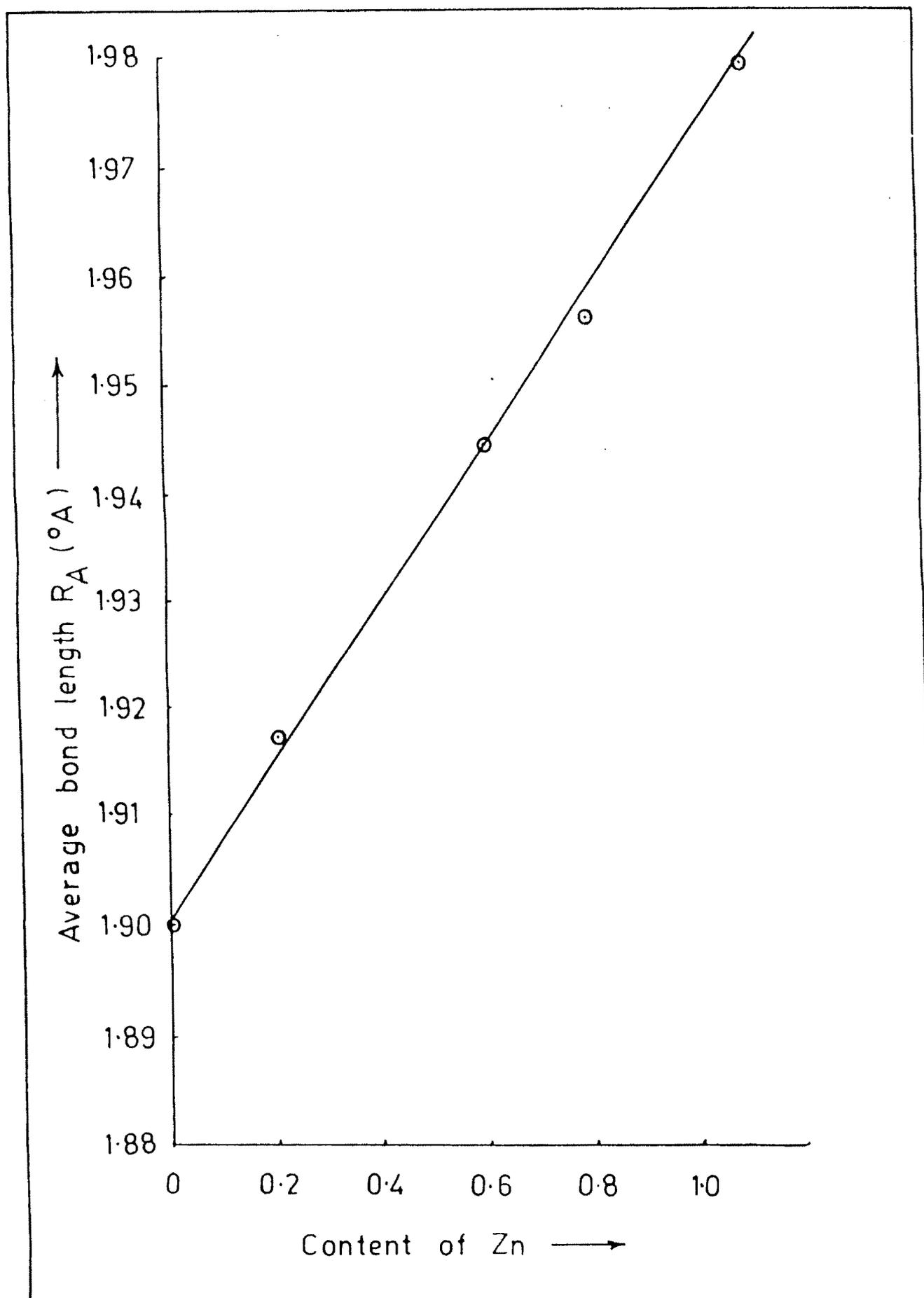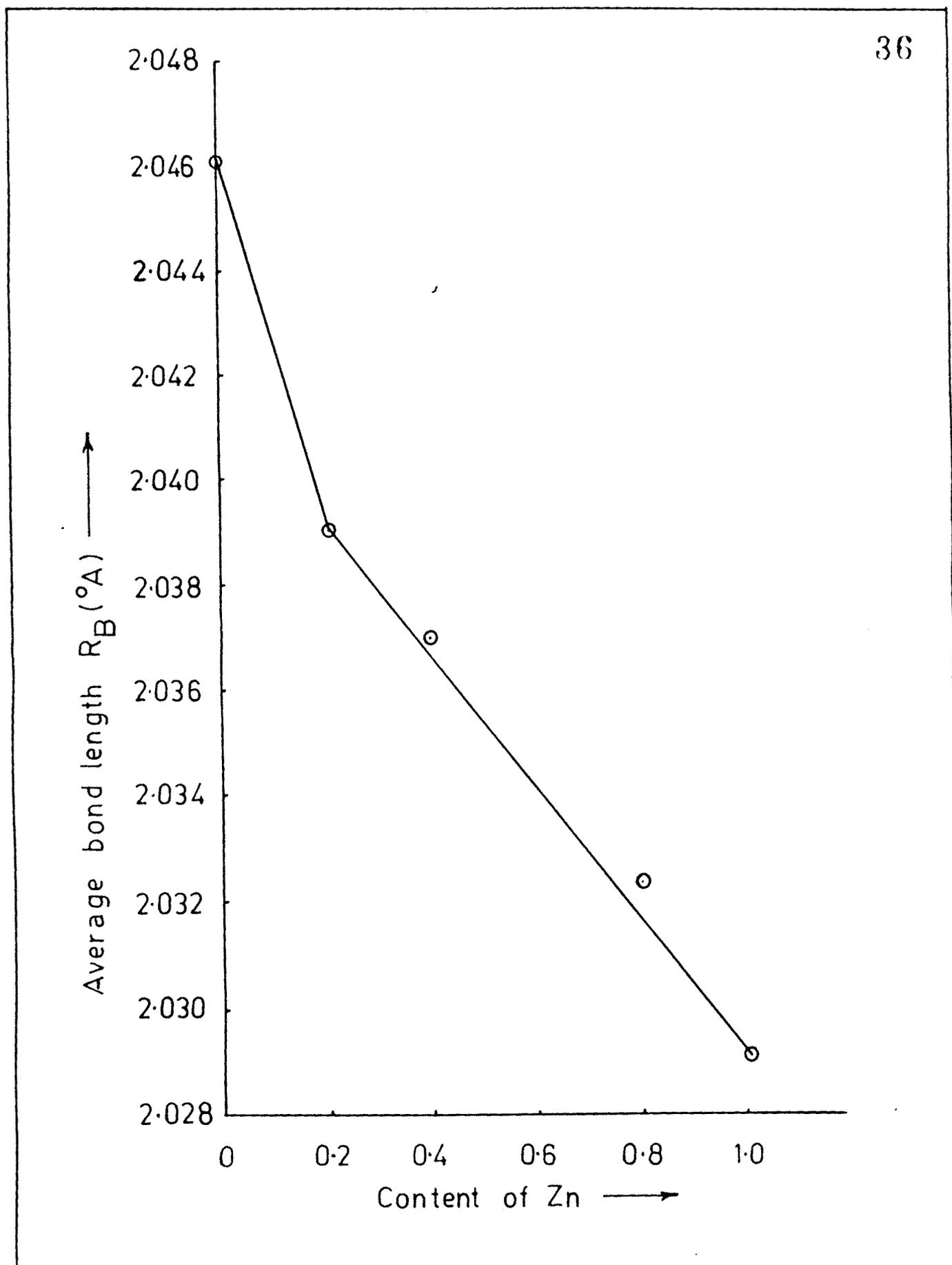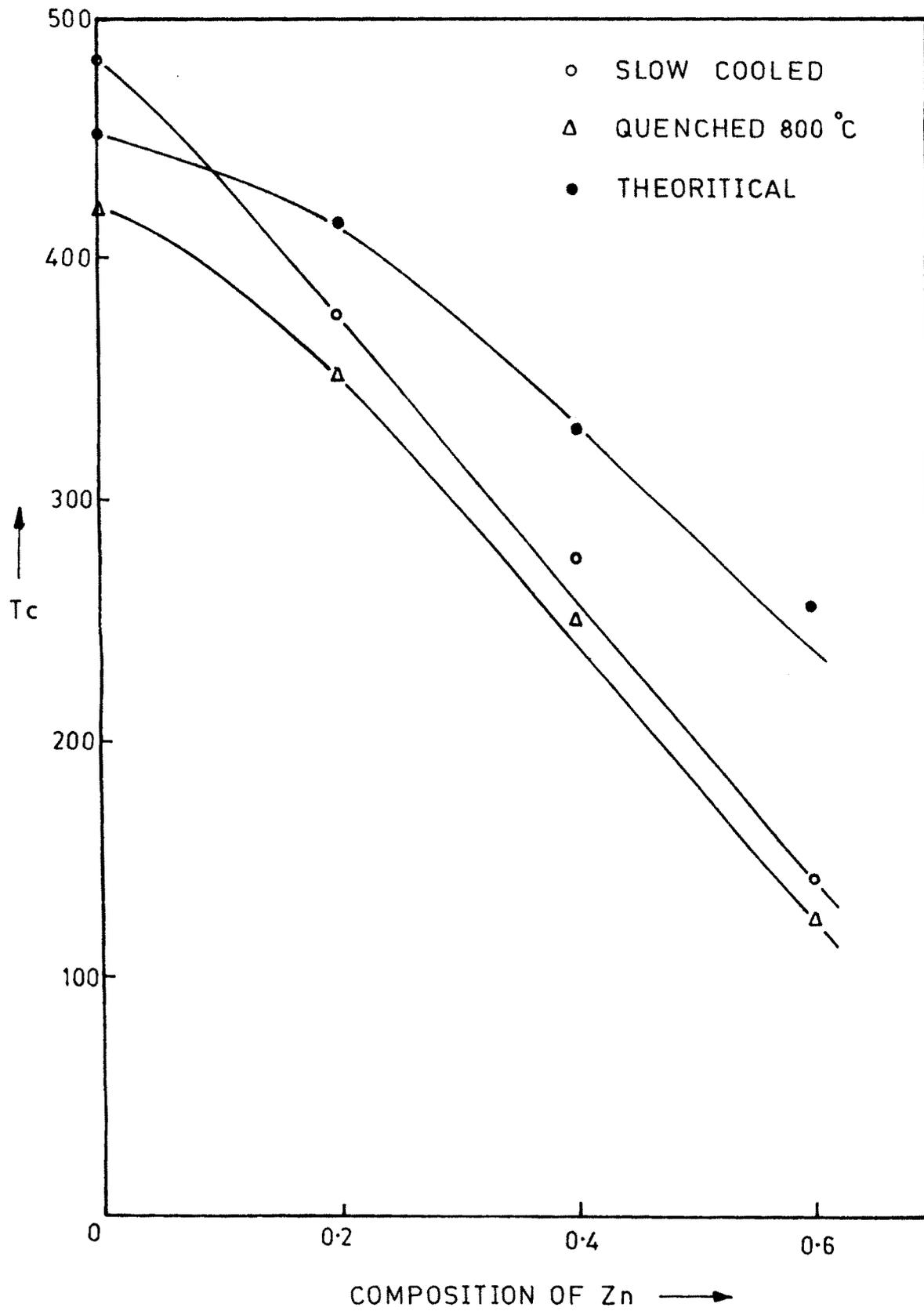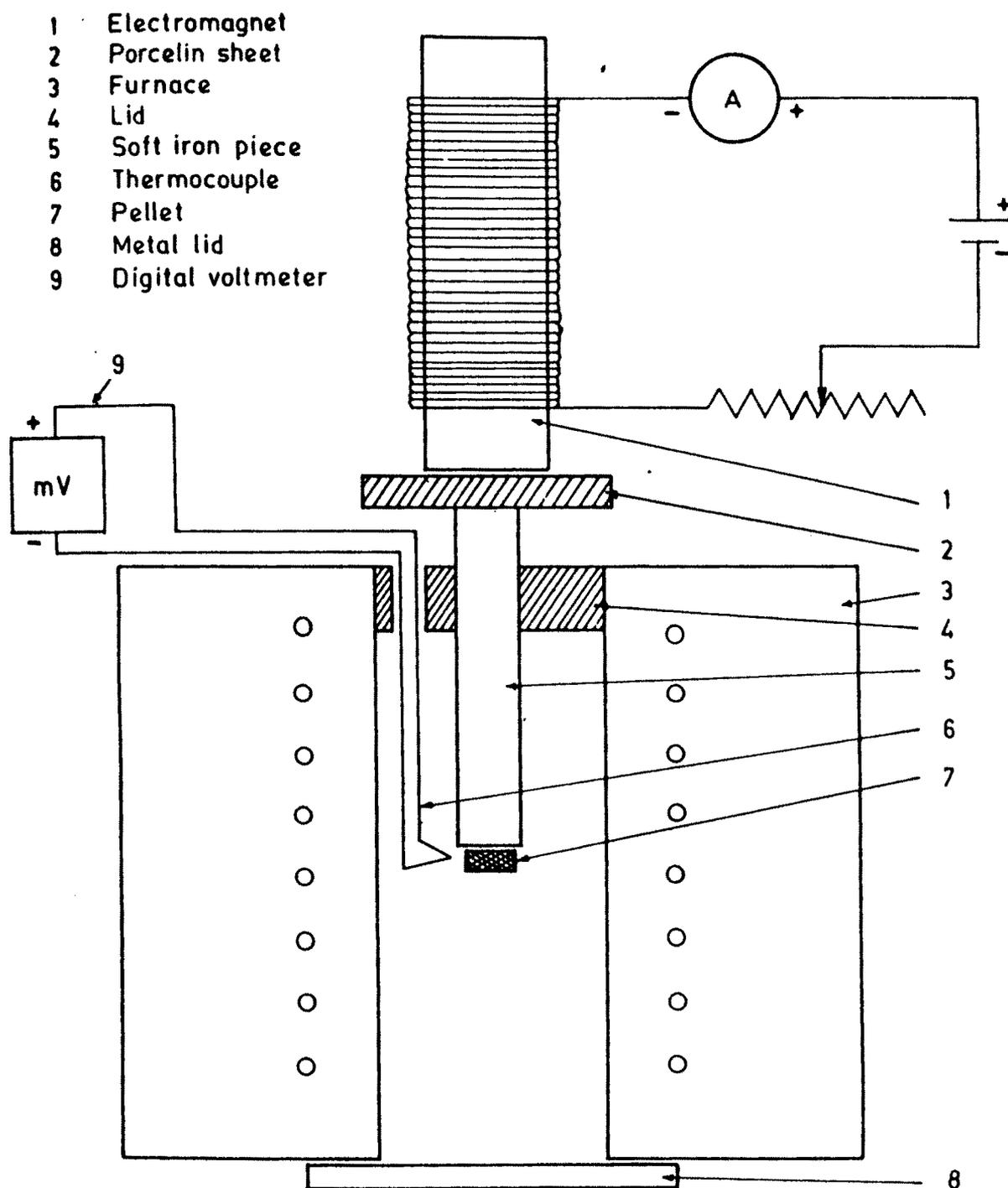
: SET UP FOR DETERMINATION OF CURIE
                    TEMPERATURE (Tc).

NOTES AND REFERENCES

1   Toshio Takada and M. Kiyamg. Ferrites Proces.
     Internat. Conf. (July 1970), Japan, 69-71.

2   Donald G. Wickhman, Ferrites, Proces. International
     Conf. (July 1970), 105-107.

3   Toshihiko Sata Chinji Kuroda and Minorce Sato.
     Ferrites, Process International Conf. (July 1970), pp. 72-74.

4   Gorter, E. (1955) Proc. IRE 42(2), 1945.

5   C. Wagner Z. Phys. Chem. B-34 (1934), pp. 309-316.

6   C.G. Kaczynski, International Conf. (1970) Japan,
     pp. 67-95.

7   Henery N.F.M., Lipson, H. and Wooster, W.A. "The
     Interpretation of X-ray Diffraction Photographs"
     Macmillan and Co. Ltd., London (1961).

8   B.D. Cullety, "Elements of X-ray Diffraction Adison
     Wesley Publishing Co. Inc. England (1959).

9   S.R. Sawant and R.N. Patil "Magnetisation and Structural
     Studies on Cu Ferrite" Indian Journal of Pure and Applied
     Physics, Vol. 21, March, 1983, pp. 145-147.

10   G.K. Joshi, S.A. Deshpande, A.Y. Khot and S.R. Sawant
     "Lattice Parameter Cation Distribution and Bond Length
     Studies of $Zn_xMg_{1-x}Fe_2O_4$ system" (Accepted for publication
     in Indian Journal of Physics, 1987).

11   Standley, K.J., Oxide Magnetic Materials Clarendon
      Press, Oxford (1972).

12   Laoria, K.K. and Sinha, A.P.B., Indian J. Pure & Appl.
      Physics 1 (1963), p. 115.

13   A.Y. Khot, "X-Ray spectroscopic Studies of Cu-Zn and
      Cu-Mg mixed Ferrites". Ph.D. thesis, Shivaji University,
      Kolhapur, 1982.

14   Standley, K.J. (1972). Oxides Magnetic Materials,
      Clarendon Press, Oxford, p. 28.

15   Levine, B.F. (1973). Phys. Rev. (USA) B-7 2591.

16   J.D. Dunitz and L.E. Orgel (1957). J. Phys. Chem.
      Solids 3 (G.B.) 318.

17   S.R. Sawant and R.N. Patil (1983) Indian Journal of
      Pure and Applied Physics 21 (India) 145-147.